Catalysis Today 149 (2010) 365–371

Contents lists available at ScienceDirect

Catalysis Today

journal homepage: www.elsevier.com/locate/cattod

Production of hydrogen and MWCNTs by methane decomposition over catalysts originated from $LaNiO_3$ perovskite

Germán Sierra Gallego [a,*], Joël Barrault [b], Catherine Batiot-Dupeyrat [b], Fanor Mondragón [c]

[a] Universidad Nacional de Colombia - Escuela de Ingeniería de Materiales, Minas - Sede Medellín, Colombia
[b] Laboratoire de Catalyse en Chimie Organique, UMR CNRS 6503, Université de Poitiers, Ecole Supérieure d'Ingénieurs de Poitiers, 40, avenue du Recteur Pineau, 86022 Poitiers Cedex, France
[c] University of Antioquia, Institute of Chemistry, Calle 67 No. 53 - 108 A.A. 1226, Medellín, Colombia

ARTICLE INFO

Article history:
Available online 25 July 2009

Keywords:
Methane decomposition
Perovskites
Carbon nanotubes
Hydrogen production

ABSTRACT

$LaNiO_3$ type perovskite was prepared by the "self-combustion" method and was used as catalyst precursor for the methane decomposition reaction at 600 and 700 °C. CH_4 conversion reaches 80% at 700 °C and 65% at 600 °C using pure CH_4. The yield of CNT and H_2 were 2.2 g_{CNT} g^{-1} h^{-1} and 8.2 L g^{-1} h^{-1} at 700 °C respectively after 4 h of reaction. When the reaction is prolonged to 22 h the catalytic activity decreases but the catalyst is still active, the production of hydrogen reaches 63.5 L (STP) per gram of catalyst and the production of MWCNT was equal to 17 g per gram of catalyst.

Multi-wall carbon nanotubes were characterized by X-ray diffraction (XRD), surface area (BET), transmission electron microscopy (TEM), scanning electron microscopy (SEM), thermogravimetric analysis (TGA) and Raman spectroscopy. TEM micrographs showed that MWCNT longer than 20 μm were formed with inner diameters ranging from 5 to 16 nm and outer diameters up to about 40 nm.

The results obtained here clearly show that the use of the perovskite $LaNiO_3$ as catalytic precursor is very effective for the simultaneous production of carbon nanotubes and hydrogen.

1. Introduction

Hydrogen is of great industrial interest, it is used in processes for the desulphurization and/or hydrogenation of aromatic derivatives produced in oil refining plants. Moreover the utilization of hydrogen for fuel-cell type applications is considered to be one of the most promising leads to answer the energy needs of the future [1]. Methane steam reforming (MSR) has been the most widely used and generally the most economical technology for the production of H_2 [2]. However, the hydrogen production is accompanied by CO formation typically with a ratio $H_2/CO = 3/1$, the reforming reaction is followed by the water gas shift reaction ($CO + H_2O \rightarrow CO_2 + H_2$) in order to remove carbon monoxide.

The thermo-catalytic decomposition of methane has been proposed as an alternative route for the production of CO/CO_2-free hydrogen [3]. The process involves the production of a very important product: carbon. Metal catalysts such as Ni, Fe, Co based catalysts have been widely used; however there is a catalyst deactivation due to the blockage of the active sites by carbon deposition. The nature of carbon thus prepared depend on the operational conditions, it could be high value filamentous carbon: multi-walled carbon nanotubes. Carbon nanotubes and carbon nanofibers have many unique properties, such as high resistance to strong acids and bases, high electric conductivity, high surface area, and high mechanical strength [4]. These unique properties result in many potential applications, such as catalyst supports, selective adsorption agents, hydrogen storage, composite materials, nano-electronic and nano-mechanical devices, and field emission devices [5].

Three technologies have been used for the synthesis of carbon nanotubes: arc discharge, laser ablation and catalytic chemical vapor deposition (CCVD). The CCVD method appears as a promising technique, the catalyst precursor being crucial to control the size and the purity of the CNT. It has been shown that the size of the active element, usually Fe, Co and Ni, can be correlated with the tubes diameter [6]. For that purpose, mixed metal oxides such as $LaFeO_3$ [7] and La_2NiO_4 [8] were used as catalyst precursor for the preparation of CNT using the CCVD method. The use of a perovskite as catalyst precursor is of great interest since its reduction leads to the formation of small nickel particles deposited on lanthanum oxide, consequently the shape of the CNT can be controlled.

The decomposition of methane, using a reduced perovskite, was mostly investigated with the goal of the production of CNT, thus a mixture of CH_4 and H_2 was used in the studies [9].

* Corresponding author at: Carrera 80 # 65-223, Bloque M3-020, Colombia. Tel.: +57 4 4255286.
E-mail address: geasierraga@unal.edu.co (G. Sierra Gallego).

0920-5861/$ – see front matter © 2009 Elsevier B.V. All rights reserved.
doi:10.1016/j.cattod.2009.06.004

The objective of this work was to show that the use of the perovskite $LaNiO_3$ as catalyst precursor is not only interesting for the production of CNT but also for the production of hydrogen in high yields. Indeed, in a recent review on hydrogen production technologies, Holladay et al. [10] assumed that the catalytic decomposition of hydrocarbon will play a significant role in the future due to the "clean" carbon formation associated with the hydrogen production. The catalytic decomposition of methane into hydrogen and carbon was studied by Shah et al. using bimetallic iron catalysts FeM (M = Pd, Mo or Ni) supported on alumina. They showed that carbon is deposited in the form of amorphous carbon, carbon flakes at high temperatures (>900 °C) whereas multi-walled nanotubes are obtained in the temperature range of 700–800 °C [11].

In this study methane was used without dilution gas. The catalyst stability was investigated by performing the reaction for 22 h. The influence of the reaction temperature was also studied.

2. Experimental

2.1. Catalysts preparation

The perovskite type oxide $LaNiO_3$ was prepared by the self-combustion method [12]. Glycine ($H_2NCH_2CO_2H$), used as ignition promoter, was added to an aqueous solution of metal nitrates with the appropriate stoichiometry in order to get a $NO_3^-/NH_2 = 1$ ratio. The resulting solution was slowly evaporated until a vitreous green gel was obtained. The gel was heated up to around 250 °C, temperature at which the ignition reaction occurs producing a powdered precursor which still contains carbon residues. Calcination at 700 °C for 8 h eliminates all of the remaining carbon and leads to the formation of the perovskite structure.

2.2. Catalytic decomposition of methane

The reaction was carried out in a horizontal reactor in order to avoid sub-pressure during the formation of CNT (Fig. 1).

About 50 mg of the catalyst was placed directly into the reactor and pre-reduced with pure hydrogen (30 mL/min) at 700 °C for 1 h. The reduced Ni/La_2O_3 catalyst was then cooled down to room temperature under helium flow. Methane (99.995% purity) was then introduced in the reactor at a rate of 15 mL/min and the reactor temperature was increased from room temperature to 600 or 700 °C at a rate of 10 °C/min, and kept at this temperature for the desired reaction time.

The gaseous reaction products were analyzed by an on-line mass spectrometer.

The produced carbon nanotubes were purified by acid treatment to dissolve the catalyst. CNT was treated with HNO_3, 65%, for 1 h under continuous stirring. The product was filtered and washed with deionized water. The residue was then dried at 100 °C for 24 h, and the CNT weight determined.

2.3. Characterization

The catalysts were characterized by powder X-ray diffraction (XRD) using a Siemens D-5000 diffractometer with $CuK_{\alpha 1}$ = 1.5406 Å and $CuK_{\alpha 2}$ = 1.5439 Å, operated at 40 kV and 30 mA. The diffraction patterns were recorded in the 2θ values range 10–90° with a step size of 0.01° and 1 s per step.

Transmission electron microscopy (TEM) was carried out on a Philips CM120 instrument, with LaB_6 filament and equipped with energy dispersive X-ray analyzer (EDX). TEM images of deposited carbon were taken after treatment of the sample with 65%-HNO_3. The sample was deposited on a Cu grid for TEM observation. Scanning electron microscopy (SEM) was carried out on JEOL JSM 840.

Raman spectra of carbon nanotubes were obtained by diluting the sample in KBr, using a PerkinElmer Spectrum GX-IR FT equipment with a diode Nd:YAG laser and a wavelength of 514.5 nm from 10 to 4000 cm^{-1}.

Thermogravimetric analysis (TGA) of CNTs was carried out in a TA Instruments 2950 equipment. Samples were placed in a platinum pan in quantities of 5–8 mg and heated at 10 °C/min from room temperature up to 900 °C under air.

Surface areas were determined using nitrogen–helium adsorption. All samples were degassed under He for 30 min at 623 K before analysis, adsorption–desorption isotherms of N_2 were determined using 30% N_2/He as adsorbate on a Micromeritics Flowsorb II 2300 apparatus at −196 °C.

3. Results and discussion

3.1. Characterization of the catalyst by electron microscopy

The authors have shown in a previous study that the reduction of $LaNiO_3$ under hydrogen at 700 °C allow the formation of small metallic Ni particles [13]. The presence of spherical particles of nickel is clearly visible on TEM micrograph (Fig. 2). The particle size distribution is reported in Fig. 3, the particle size ranged between 2 and 50 nm. The average size of metallic particles was calculated using the following equation: $d = \sum_i n_i d_i^3 / \sum_i n_i d_i^2$.

Where n_i is the particle number and d_i is the characteristic diameter of particles [14]. The average particle size is around 15 nm.

This result suggests that the use of the well defined crystallized perovskite $LaNiO_3$ as catalyst precursor, allows to prevent

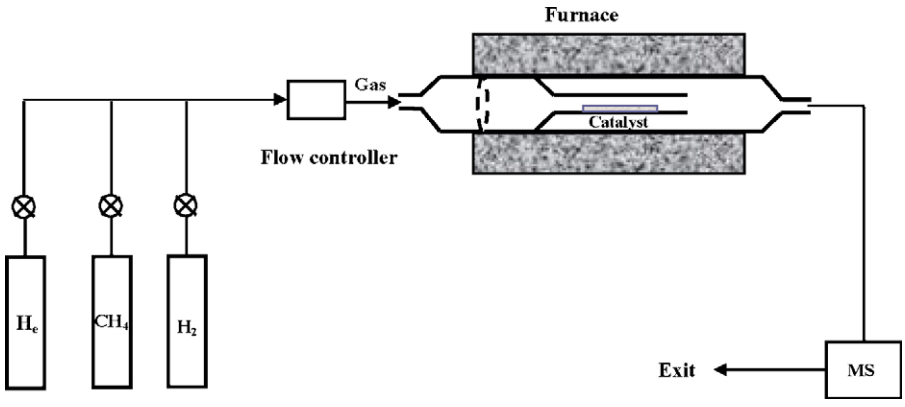

Fig. 1. Schematic diagram of experimental apparatus for methane decomposition.

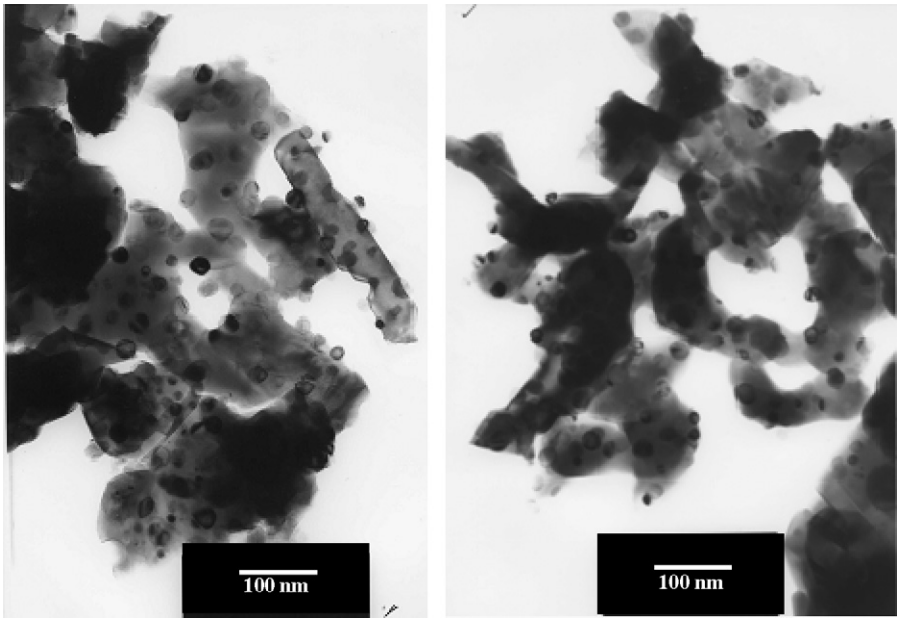

Fig. 2. TEM micrograph obtained after reduction of $LaNiO_3$ under hydrogen at 700 °C.

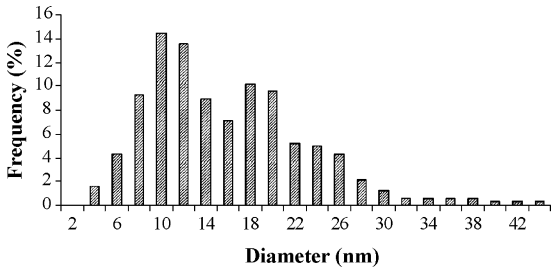

Fig. 3. Ni particle size distribution determined from TEM micrographs of $LaNiO_3$ reduced under hydrogen at 700 °C.

agglomerations of the transition metal and promotes the dispersion of nano-scale Ni particles, which has been reported as a very advantageous condition for CNT growth [15].

3.2. Catalytic decomposition of methane

The catalytic decomposition of methane was performed at two different temperatures, at 600 and 700 °C. The reaction was preformed during 4 and 22 h in order to observe the catalyst deactivation.

3.2.1. Influence of the reaction temperature

Fig. 4 depicts the experimental results of methane catalytic decomposition at 700 and 600 °C. Whatever the reaction conditions hydrogen was the only product formed during the reaction, which is in accordance with previous studies [16–18].

Methane conversion increases slowly during the rise of temperature. As soon as 600 °C is reached the conversion of methane is maximum (around 60%) and remains almost constant during the following 4 h of reaction. At 700 °C, the methane conversion reaches 80% which is very close to the thermodynamic value, then the CH_4 conversion decreases slowly during the reaction, after 4 h the conversion is equal to 60%. In our knowledge, the values obtained here are among the highest single pass conversions of methane reported for this process [19–21].

In order to compare our results with those of the literature, yields of CNT and H_2 obtained using different nickel based materials are gathered in Table 1. Most of the studies were performed in order to produce CNT, so the yield of hydrogen is often missing. Moreover the yield of CNT is often given after the complete deactivation of the catalysts, so in order to compare the catalytic activity of the different materials, the yield of CNT was indicated per gram of catalyst and per hour.

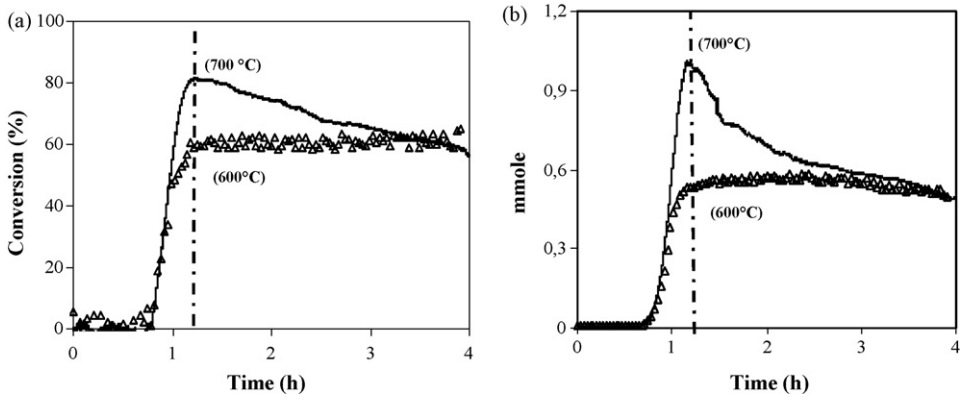

Fig. 4. (a) Conversion of CH_4 and (b) H_2 yield at 700 and 600 °C using Ni^0/La_2O_3 obtained from $LaNiO_3$ perovskite. CH_4 flow = 15 mL/min and 50 mg of catalyst.

Table 1
Comparison of methane conversion, yield of CNT and H_2 at different conditions, between our catalyst and those reported in the literature.

Catalyst	Ni^0%	Temp (°C)	Conc. CH_4 in feed (%)	Max. CH_4 conv (%)	Yield of H_2 ($L\,g^{-1}\,h^{-1}$)	$g_{CNT}\,g^{-1}\,h^{-1}$	Ref.
Ni/La_2O_3	23	700	100	80	8.2	2.20	This work
Ni/La_2O_3	23	600	100	65	7.5	2.02	This work
Ni/MgO	48	550	10	38		0.7	22
Ni/SiO_2	16	550	10	35		0.8	
Ni/ZrO_2	55	550	10	4		0.2	
$Ni/LiAlO_2$	16	550	10	35		0.6	
$Ni–Cu–Al_2O_3$	Ni = 45–90	625	100	22		8.4	23
	Cu = 8–45	675	100	35		11.1	
$65Ni–25Cu–10Nb_2O_5$	65	600	100	45	50	6.9	24

Table 2
Methane conversion and yields of CNT and H_2 at different reaction times and temperatures using the catalyst obtained from the $LaNiO_3$ perovskite.

Catalyst	Temp (°C)	Time of reaction (h)	Max. CH_4 conv (%)	Yield of H_2 ($L\,g^{-1}\,h^{-1}$)	Yield of H_2 ($L\,g_{cata}^{-1}$)	$g_{CNT}\,g^{-1}\,h^{-1}$	$g_{CNT}\,g_{cata}^{-1}$
Ni/La_2O_3	700	4	80	8.2	32.3	2.20	8.7
Ni/La_2O_3	600	4	65	7.5	29.9	2.02	8.0
Ni/La_2O_3	700	22	75	2.9	63.5	0.85	17.0

The results obtained by Bonura et al. [22], using different supports of nickel showed that a strong deactivation proceed. After 4 h of reaction the catalyst Ni/MgO is completely deactivated, whereas Ni/ZrO_2, $Ni/LiAlO_2$, Ni/SiO_2 are no more active after 1, 2 and 3 h of reaction respectively. In these works, the formation of filamentous and encapsulating carbon species was showed, being the last species the responsible for catalyst deactivation. The production of carbon was lower than the one we obtained using the perovskite $LaNiO_3$ as catalyst precursor.

The use of bimetallic copper–nickel system supported on alumina was reported by Reshetenko et al. [23]. The addition of a low amount of copper in the $Ni–Al_2O_3$ catalysts acts as a stabilizing component, the catalyst lifetime being increased. An increase of the temperature reduces the catalyst lifetime; the methane conversion at 675 °C is higher than which at 625 °C but it sharply decreases after 5 h of reaction. TEM analysis reveals the presence of encapsulating carbon species.

Niobium oxide was used as bimetallic nickel–copper support for methane decomposition to hydrogen and filamentous carbon by Li et al. [24]. The maximum yield of hydrogen was obtained for $65Ni–25Cu–5Nb_2O_5$, as shown in Table 1 high yields are obtained. Nevertheless, TEM images after 18 h of reaction reveals the presence of very small filaments in length, suggesting that the filament are very fragile.

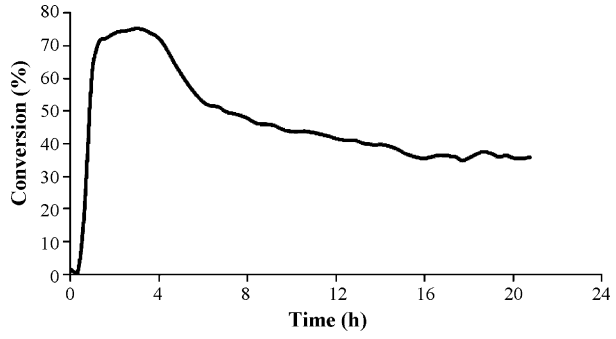

Fig. 5. CH_4 conversion during 22 h of reaction at 700 °C using Ni^0/La_2O_3 obtained from $LaNiO_3$ perovskite. CH_4 flow = 15 mL/min and 50 mg of catalyst.

3.2.2. Influence of the time of reaction

The catalytic decomposition of methane over catalyst obtained from $LaNiO_3$ precursor was performed during 22 h of reaction at 700 °C. The evolution of methane conversion is reported in Fig. 5. The conversion sharply increases to reach 75% and then a slow decrease is observed. After 20 h of reaction, the catalyst is still active being the CH_4 conversion equal to 40%. The yield of hydrogen and carbon is reported in Table 2, after 22 h of reaction high yields of hydrogen and CNT per gram of catalyst are obtained, which shows that $LaNiO_3$ used as catalyst precursor is an interesting material for the simultaneous production of CNT and hydrogen.

3.3. CNTs characterization

3.3.1. BET and CHN analysis

The specific surface area of the purified CNTs measured by N_2 adsorption was equal to 81 $m^2\,g^{-1}$. Some authors proposed that acid purification can partially open the CNT tips and remove the metallic particles from them increasing the BET surface [25].

Elemental analysis of the CNTs showed that the composition of the material corresponds to: carbon 99.1% and hydrogen 0.9%.

3.3.2. Characterization of CNTs by transmission electron microscopy

TEM micrographs provided clear evidence of the formation of multi-wall carbon nanotubes during the methane decomposition reaction (Fig. 6). We can see many rope-like structures of carbon nanotubes with several microns in length. The inner diameters ranging from 5 to 16 nm and outer diameters up to about 40 nm. The inner diameters are very close to the previously determined size of the Ni particles. Most of the Ni particles capped nanotube tips or were encapsulated by the CNT.

Similar shapes of the CNT are shown in the literature using catalysts such as NiO [26], $NiAl_2O_4$ [27] and $Ni/Cu/Al_2O_3$ [28].

TEM micrographs performed after 22 h of reaction (Fig. 7) shows the presence of MWCNT longer than 20 μm in a high amount. The growth of the nanotube is thus facilitated using the catalyst obtained from $LaNiO_3$ precursor. The MWCNT formed are particularly resistant since they are not broken in to pieces when the reaction is extended to 22 h. This result is very interesting since it is shown in the literature that CNT can be fragile when the reaction is performed during 18 h using a $Ni/Cu/Nb_2O_5$ catalyst [29].

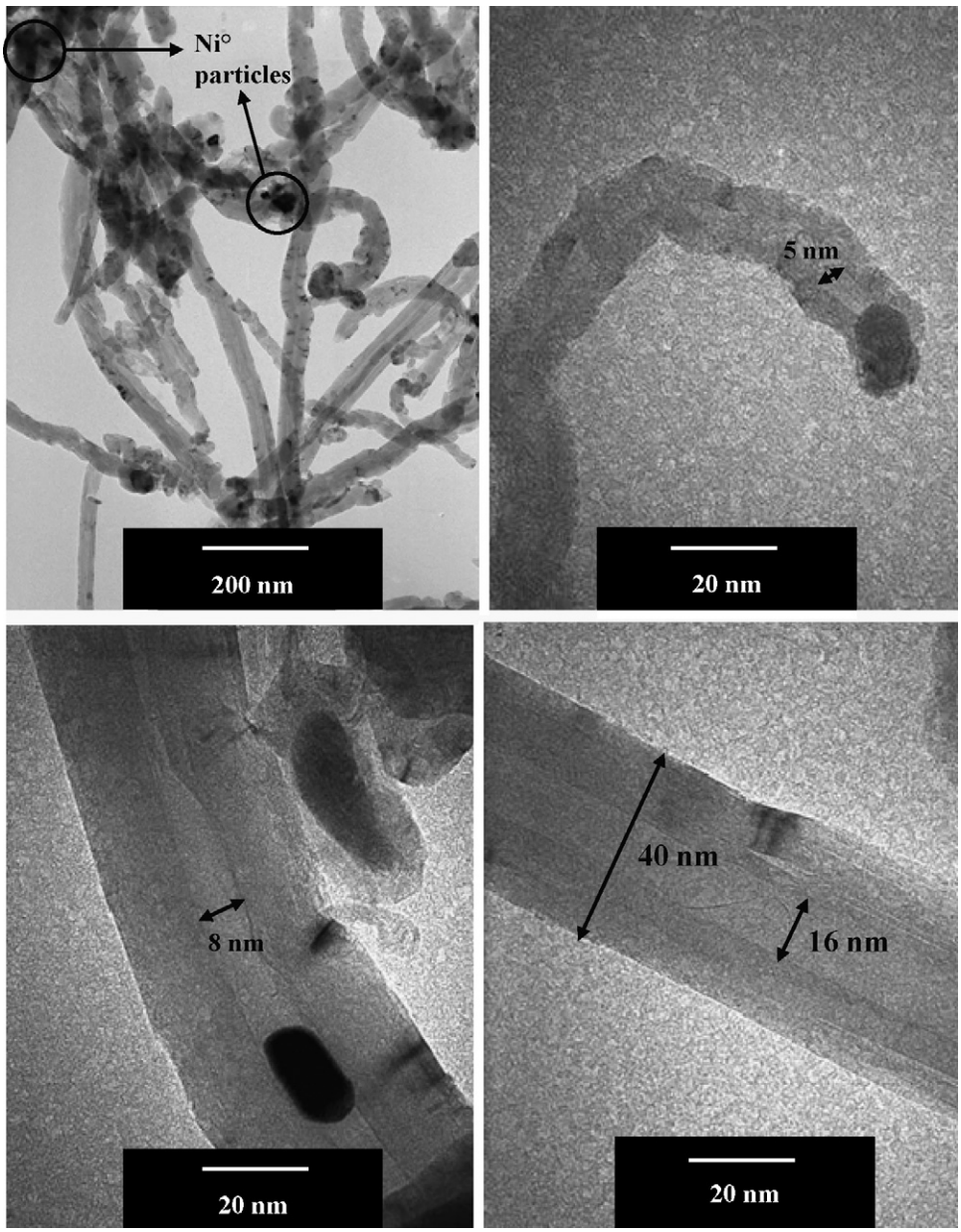

Fig. 6. TEM micrographs of multi-wall carbon nanotubes obtained after 4 h of reaction and after treatment with 65%-HNO_3.

3.3.3. Thermogravimetric characterization of MWCNTs

After reaction the MWCNTs were purified by treatment with HNO_3-65% in order to remove the catalyst particles. Then, to remove amorphous carbon an oxidation treatment with H_2O_2 was carried out. In this step there was no weight loss suggesting that the content of amorphous carbon in the product was insignificant [30]. After purification thermogravimetric analysis was carried out to study the oxidation behavior of CNT. The analysis was performed with a heating rate of 10 °C/min up to 800 °C in air. The oxidation profile is presented in Fig. 8.

An initial weight loss (0.05 wt%) from ambient temperature to 200 °C, for the sample, is attributed to the removal of physisorbed water. A second weight loss of 1.2 wt% between 200 and 550 °C can be attributed to the burning of amorphous carbon on the outer wall of nanotubes and some surface structure defects [31,32]. This total weight loss up to a temperature of 550 °C is less than 2 wt%, suggesting that the amount of disordered carbon sample is very low.

Complete oxidation of the sample takes place between 550 and 750 °C. The residue found after complete oxidation of carbon species is 5.0 wt% of the original sample. Assuming that the residue after oxidation is just NiO, this suggests that about 80% the Ni in the perovskite was encapsulated inside the CNT's, which indicates a very high availability of Ni metal for the growth of CNT when Ni–perovskite is used as precursor.

The temperature of oxidation of CNT is almost equal to the value reported by Ajayan (over 700 °C) [33] and higher than that of Kukovitskii (ca. 420 °C) [34]. Thus purity of MWCNTs in the optimal processing condition is estimated as over 94%.

3.3.4. Raman characterization of CNTs

Raman spectrum of the carbon nanotubes after acid treatment is shown in Fig. 9. The spectrum presents bands originated from carbon structures. The band at 1602 cm^{-1} is due to the tangential C–C stretching (G mode), at the one at 1290 cm^{-1} is the D mode, attributed to disordered carbon structures present in carbon

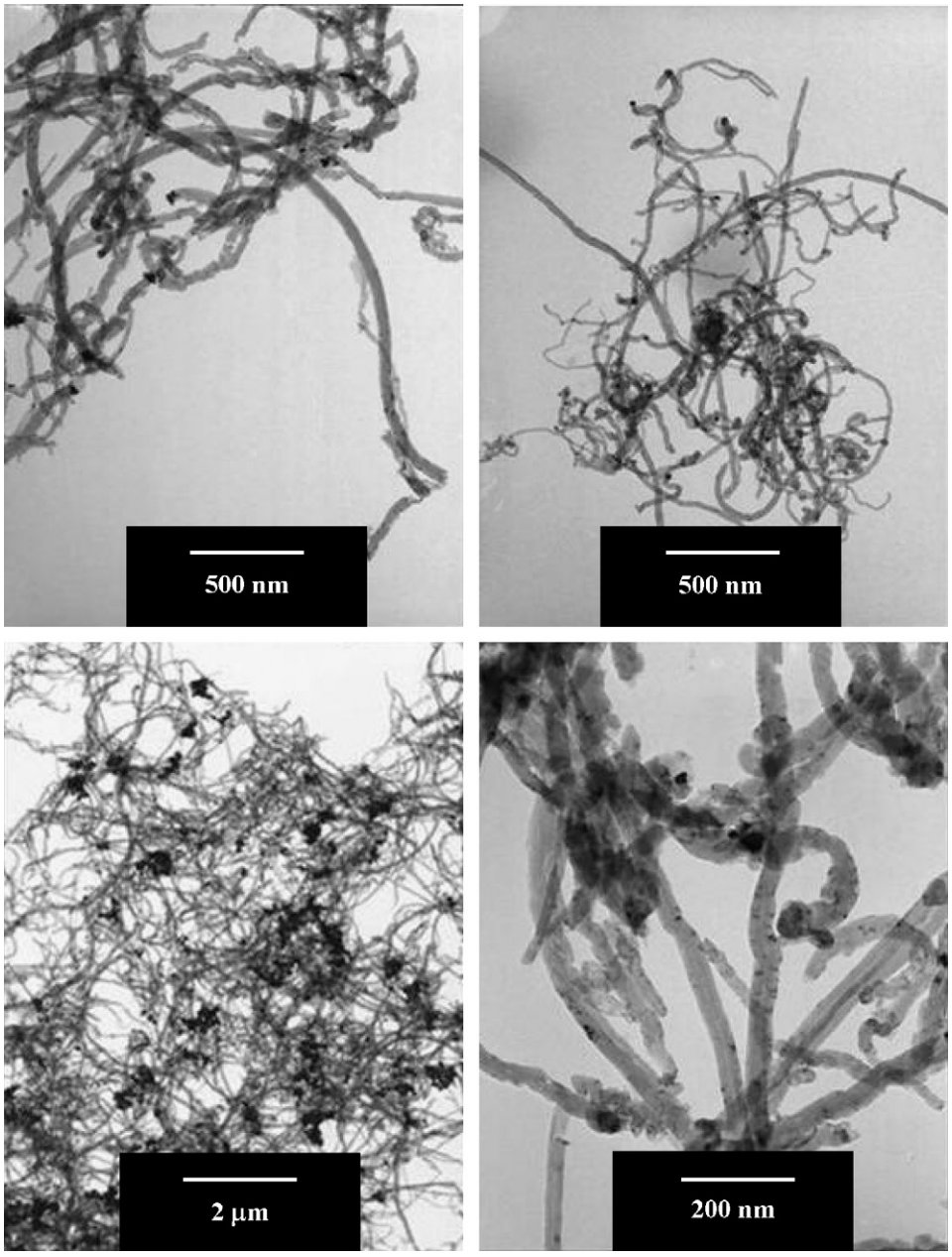

Fig. 7. TEM micrographs of multi-wall carbon nanotubes obtained after 22 h of reaction and after treatment with 65%-HNO_3.

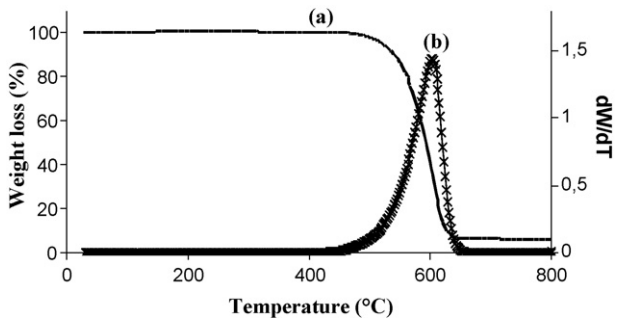

Fig. 8. (a) TGA of carbon nanotubes after treatment with 65%-HNO_3. (b) Derivative TG curves of (a).

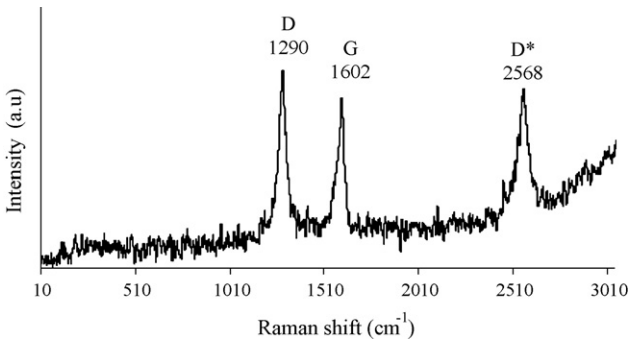

Fig. 9. Raman spectrum of carbon nanotubes after treatment with 65%-HNO_3.

nanotubes or other carbon forms, with its overtone at 2568 cm^{-1}. The relative intensity of the ratio I_D/I_G can express the graphitization of carbon nanotubes or degree of disorder in the structure, which is related to the quality of the carbon nanotubes. Tan et al. [35] reported values of $I_D/I_G = 0.051$ for highly oriented pyrolytic graphite (highly organized), $I_D/I_G = 0.430$ for carbon nanotubes prepared by D.C. arc discharge and $I_D/I_G = 3.56$ for CNT prepared by catalytic methods. In our case $I_D/I_G = 1.15$, indicating that the carbon nanotubes are quite well graphitized. This is confirmed by the oxidation temperature observed by TGA.

4. Conclusions

The reduction of the perovskite $LaNiO_3$ leads to the formation of small nickel particles with an average diameter of 15 nm. This catalyst presents a high activity for the methane decomposition reaction. CH_4 conversion reaches 80% at 700 °C and 65% at 600 °C using pure CH_4. The yield of CNT and H_2 were 2.2 $g_{CNT}\ g^{-1}\ h^{-1}$ and 8.2 L $g^{-1}\ h^{-1}$ at 700 °C respectively after 4 h of reaction. When the reaction is prolonged the catalytic activity decreases but the catalyst is still active after 22 h of reaction, the production of hydrogen reaches 63.5 L (STP) per gram of catalyst and the production of MWCNT was equal to 17 g per gram of catalyst.

The MWCNT had inner diameters ranging from 5 to 16 nm and outer diameters up to about 40 nm. After 22 h of reaction TEM micrographs revealed that CNT longer than 20 μm are formed in a large amount, showing that the growth of CNT is favored using the catalyst obtained from $LaNiO_3$ precursor. The destruction of CNT does not seem to proceed in our experimental conditions when the reaction time is increased.

The results here obtained clearly show that the use of the perovskite $LaNiO_3$ as catalytic precursor is very effective for the simultaneous production of carbon nanotubes and hydrogen.

Acknowledgements

The authors are grateful to Colciencias and the University of Antioquia for the support of the project 1115-06-17639. F. Mondragon and G. Sierra thank the University of Antioquia for the financial support of the Sostenibilidad program and G. Sierra would like to thank Colciencias and the University of Antioquia for the PhD scholarship.

References

[1] N.Z. Muradova, T.N. Veziroglub, Int. J. Hydr. Energy 30 (2005) 225.
[2] J.N. Armor, Appl. Catal. A: Gen. 189 (1999) 153.
[3] N.Z. Muradov, Int. J. Hydr. Energy 18 (1993) 211.
[4] S. Xie, W. Li, Z. Pan, B. Chang, L. Sun, J. Phys. Chem. Solids 61 (2000) 1153.
[5] K. Lozano, E.V. Barrera, Appl. Polym. Sci. 79 (2001) 125.
[6] H. Dai, P. Nikolaev, A. Thess, A.G. Rinzler, D.T. Colbert, R.E. Smalley, Chem. Phys. Lett. 260 (1996) 471.
[7] B.C. Liu, S.H. Tang, Chem. Phys. Lett. 357 (2002) 297.
[8] Q. Liang, L.Z. Gao, Q. Li, Carbon 39 (2001) 897.
[9] M. Kuras, Y. Zimmermann, C. Petit, Catal. Today 138 (2008) 55.
[10] J.D. Holladay, J. Hu, D.L. King, Y. Wang, Catal. Today 139 (2009) 244.
[11] N. Shah, D. Panjala, G. Huffman, Energy Fuels 15 (2001) 1528.
[12] R. Pechini, US Patent No 3330 697 (1967) Method of preparing lead and alkaline earth titanates and niobates and coating method using the same to form a capacitor.
[13] G. Sierra Gallego, F. Mondragón, J. Barrault, J.-M. Tatibouët, C. Batiot-Dupeyrat, Appl. Catal. A: Gen. 311 (2006) 164.
[14] D.G. Mustard, C.H. Bartholomew, J. Catal. 67 (1981) 186.
[15] Z.W. Pan, S.S. Xie, B.H. Chang, L.F. Sun, W.Y. Zhou, G. Wang, Chem. Phys. Lett. 299 (1999) 97.
[16] L.B. Avdeeva, D.I. Kochubey, S.K. Shaikhutdinov, Appl. Catal. A 177 (1999) 43.
[17] R. Aiello, J.E. Fiscus, H.C.Z. Loye, M.D. Amiridis, Appl. Catal. A 192 (2000) 227.
[18] W.Z. Qian, T. Liu, F. Wei, Z.W. Wang, H. Yu, Carbon 41 (2003) 846.
[19] T.V. Reshetenko, L.B. Avdeeva, Z.R. Ismagilov, A.L. Chuvilin, V.B. Fenelonov, Catal. Today 102–103 (2005) 115.
[20] Q. Weizhong, L. Tang, W. Zhanwen, W. Fei, L. Zhifei, L. Guohua, et al. Appl. Catal. A: Gen. 260 (2004) 223.
[21] H. Ago, N. Uehara, N. Yoshihara, M. Tsuji, M. Yumura, N. Tomonaga, et al. Carbon 44 (2006) 2912.
[22] G. Bonura, O. Di Blasi, L. Spadaro, F. Arena, F. Frusteri, Catal. Today 116 (2006) 298.
[23] T.V. Reshetenko, L.B. Avdeeva, Z.R. Ismagilov, A.L. Chuvilin, V.A. Ushakov, Appl. Catal. A: Gen. 247 (2003) 51.
[24] J. Li, G. Lu, K. Li, W. Wang, J. Mol. Catal. A: Chem. 221 (2004) 105.
[25] S. Porro, S. Musso, M. Vinante, L. Vanzetti, M. Anderle, F. Trotta, A. Tagliaferro, Phys. E: Low-dimens. Syst. Nanostruct. 37 (2007) 58.
[26] Y. Li, B. Zhang, X. Xie, J. Liu, Y. Xu, W. Shen, J. Catal. 238 (2006) 412.
[27] L. Piao, Y. Li, J. Chen, L. Chang, J.Y.S. Lin, Catal. Today 74 (2002) 145.
[28] Q. Weizhong, L. Tang, W. Zhanwen, W. Fei, L. Zhifei, L. Guohua, L. Yongdan, Appl. Catal. A: Gen. 260 (2004) 223.
[29] J. Li, G. Lu, K. Li, W. Wang, J. Mol. Catal. A 221 (2004) 105.
[30] J. Wang, R. Wang, X. Yu, J. Lin, F. Xie, K. Wei, J. Natural Gas Chem. 15 (2006) 211.
[31] N. Das, A. Dalai, J.S. Soltan Mohammadzadeh, J. Adjaye Carbon 44 (2006) 2236.
[32] A. Misra, P.K. Tyagi, M.K. Singh, D.S. Misra, Diam. Relat. Mater. 15 (2006) 385.
[33] P.M. Ajayan, T.W. Ebbesen, T. Ichihashi, S. Iijima, K. Tanigaki, H. Hiura, Nature 362 (1993) 522.
[34] E.F. Kukovitskii, L.A. Chernoszatonskii, Chem. Phys. Lett. 266 (1997) 323.
[35] P. Tan, S. Zhang, K. To Yue, F. Huang, J. Raman Spectrosc. 28 (1997) 369.